

INTEGRATED OPTICS

https://doi.org/10.1070/QEL16001

Abnormal blocking of a guided mode propagating in a silicon optical waveguide with periodic tunnel coupling

E.A. Kolosovskii, A.V. Tsarev

Abstract. **This paper considers abnormal blocking of a guided mode propagating in a silicon optical waveguide with periodic tunnelling inserts. Using an independent two-dimensional analysis by the method of lines (MoL) and direct simulation by the finite-difference time-domain (FDTD) method, we have identified additional signal blocking bands, unrelated to Bragg conversion to backward guided modes of the parent silicon waveguide. These bands are due to the conversion of the incident wave energy to a leaky quasi-mode of the periodically segmented structure, which subsequently transfers the energy to the ambient medium in the form of radiation modes. A distinctive feature of this phenomenon is resonant coupling of the guided mode of the strip waveguide with its radiation modes, which is due to the weak tunnel coupling with the periodically segmented structure. This structure does not support independent guided propagation, so the energy stored in it is re-emitted to space. The abnormal blocking effect may find application in optical telecommunications elements and in the fabrication of optical sensors.**

Keywords: *silicon photonics, integrated optics, optical waveguide, diffraction grating, segmented waveguide, method of lines, finite-difference time-domain method, nanophotonics.*

1. Introduction

Tunnel coupling in optical elements is used in designing various integrated optical devices for a wide range of practical applications [1, 2]. In the last decade, silicon photonics has joined the ranks of the most in-demand technology platforms for the development and fabrication of photonic elements and devices [3–5]. Optical tunnelling through an oxide buffer layer between a thick polymer waveguide and a tapered silicon waveguide in the form of photonic wire is used to ensure efficient coupling of the latter with optical fibre [6]. A similar approach was recently proposed for an efficient crossing of silicon photonic wires, a process in which an optical wave tunnels upwards and back between tapered parts of a thin single-mode silicon waveguide and thick two-mode polymer waveguide, which ensures that the wave rounds the intersection region at a low level of parasitic scattering [7, 8]. Such a technological approach can ensure multiple (up to hundreds of) crossings of small silicon waveguides with low added losses in a wide range of optical wavelengths [8] and find application in the fabrication of optical filters and multiplexers based on coupled waveguides [9, 10].

Note that, in the case of an optical wave propagating along a silicon wire, upper intermediate polymer waveguides work as periodic segmental inserts (Fig. 1). It is known that, acting as a diffraction grating, such inserts can cause efficient Bragg reflection of a guided mode in the reverse direction at certain wavelengths, thus terminating the propagation of the guided optical mode in the forward direction. As a consequence, in the case of multiple crossings the structural parameters and operating range of intersecting silicon wires in optical microchips should be chosen with allowance for the possible backreflection of the forward signal of the guided wave due to tunnel coupling with the periodic segmental polymer inserts described previously [8, 9]. Otherwise, signal propagation can be distorted.

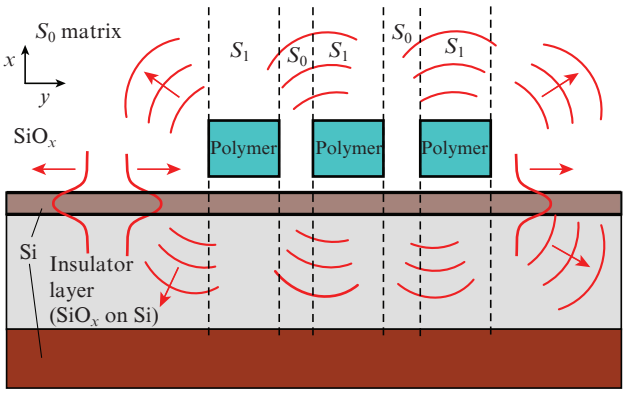

Figure 1. Schematic of the tunnelling scattering of a guided mode by periodic polymer strips for modelling by the method of lines (using *S* matrices).

Our results indicate that, in addition to the known effect of Bragg reflection to a backward guided mode [11, 12], this structure (Fig. 1) can lead to an unusual effect: abnormal blocking of forward wave propagation in which the wave reflected to the backward guided mode is essentially missing or considerably suppressed [13]. We interpret this as a manifestation of resonance tunnel coupling of the guided mode of

E.A. Kolosovskii, A.V. Tsarev A.V. Rzhanov Institute of Semiconductor Physics, Siberian Branch, Russian Academy of Sciences, prosp. Akad. Lavrent'eva 13, 630090 Novosibirsk, Russia; e-mail: kolos@isp.nsc.ru, tsarev@isp.nsc.ru

Received 11 December 2015; revision received 10 June 2016
Kvantovaya Elektronika **47** (1) 58–64 (2017)
Translated by O.M. Tsarev

the silicon wire with a virtual leaky mode of the segmented polymer waveguide based on periodic dielectric polymer inserts.

Periodically segmented waveguides are widely known in the scientific literature [14] and usually have the form of a grating structure with a completely etched core of the parent optical waveguide. The technology of such structures is well developed. As a rule, use is made of reactive ion etching (RIE), which is widely employed in micro- and nanoelectronics, as well as in the fabrication of optical waveguides, including polymer waveguides [15–17]. Segmented waveguides differ in optical properties, depending on the ratio of the grating period Λ to the optical wavelength λ_0. They can cause [14]

scattering into radiation modes;

Bragg reflection of guided modes; and

propagation of a low-loss optical wave in a subwavelength grating (SWG) structure.

The first case is basic to the fabrication of efficient grating coupler elements for light coupling into and outcoupling from a waveguide [18–20]. Such waveguides can also be used for ensuring mode selection in wide strip and grating loaded quasi-single-mode waveguides in high refractive index contrast structures [21].

Segmented Bragg-reflection waveguides are used in the fabrication of Bragg reflectors in distributed feedback lasers [22, 23], as well as in band rejection filters [24–26].

Subwavelength grating structures find combined application in silicon photonics: from controlling (engineering) the properties of optical waveguides to enhancing the functional capabilities of optical elements (from grating coupling elements to optical waveguide crossings [14]).

In this work, using numerical simulation techniques we analyse tunnel coupling of optical fields of silicon wire with a periodically segmented waveguide operating in light scattering mode at $\Lambda > \lambda_0/2$. We find and describe conditions under which a periodically segmented structure exhibits properties of a virtual (artificial) leaky waveguide ensuring abnormal blocking of the propagation of an incident guided mode without backscattering into an oppositely directed guided wave (as is characteristic of Bragg reflection).

2. Blocking of an optical wave by vertical tunnel coupling with a periodically segmented structure

The abnormal blocking effect is well observed for relatively long grating structures with a large number ($M > 300$) of periodic inserts that form a segmented waveguide and have weak tunnel coupling with an adjacent high-index silicon waveguide (Fig. 1). In this work, our analysis is limited to a two-dimensional (2D) case of a parent three-dimensional problem, which is treated here using the effective index method (EIM) [27]. We used our home-written software [8] based on the semianalytical matrix method of lines (MoL) [28], which showed itself to good advantage in solving such problems [8, 29, 30]. The results obtained with the algorithm of the method of lines were verified independently using direct numerical simulation by the finite-difference time-domain (FDTD) method [31] with RSoft-SYNOPSYS licensed software [32].

According to the approach underlying the method of lines [28], a complete solution for the x transverse field in each homogeneous z-axis-extended layered medium can be written in analytical matrix form as

$$\begin{bmatrix}\psi_1\\ \cdot\\ \cdot\\ \psi_N\end{bmatrix} = \exp\left\{\mathrm{j}\begin{bmatrix}s_{11} & \cdots & s_{1N}\\ \cdot & & \cdot\\ \cdot & & \cdot\\ s_{N1} & \cdots & s_{NN}\end{bmatrix}z\right\}\begin{bmatrix}a_1\\ \cdot\\ \cdot\\ a_N\end{bmatrix}$$

$$+\exp\left\{-\mathrm{j}\begin{bmatrix}s_{11} & \cdots & s_{1N}\\ \cdot & & \cdot\\ \cdot & & \cdot\\ s_{N1} & \cdots & s_{NN}\end{bmatrix}z\right\}\begin{bmatrix}b_1\\ \cdot\\ \cdot\\ b_N\end{bmatrix} = \exp(\mathrm{j}Sz)A + \exp(-\mathrm{j}Sz)B. \quad (1)$$

Here, A and B are columns of coefficients for forward and reverse waves, respectively. Owing to this notation, one can make formal mathematical calculations for a sequence of layered media or their alternation [30]. Between any two (vertical) boundaries, the matched amplitudes A and B have a clear meaning of a forward and a reflected wave. The large propagation matrix S (as the main characteristic of the scattering problem) can be found numerically and fully determines all possible solutions in each layered region.

Along with the analytical capabilities of the matrix exponential, the strong point of the MoL approach is that it automatically takes into account optically contrast dielectric permittivity boundaries, because the boundaries are always included in the x_j ($j = 1 \ldots N$) grid for the $\psi(x_j, z)$ field. Solution transfer across the $x_j \pm 0$ boundary is rigorous and is fulfilled for the ψ_j fields together with all four derivatives (as in our implementation of the MoL), which are extracted using differentiation of the starting wave equation. In the case of orthogonal (TE and TM) polarisations, the S matrices differ. For a given layered region, the S matrix is calculated once. For example, for the structure with alternating regions in Fig. 1, it is sufficient to calculate just two matrices (S_0 and S_1) once (as shown in Fig. 1), independent of the number of polymer inserts.

In this work, we used a modified MoL with a variable x_j step and an arbitrary number M of periodically alternating segments. To speed up computation, the number of segments used in the MoL is typically $M = 2^N$. The scattering problem then reduces to the simplest recurrent expressions over S matrices and reflection/transmission matrices of individual segments [30]. To implement the MoL algorithm, an arbitrary number of segments, M, was expanded into a power series in 2 and the complete solution of the problem was found using (1) via the analytical summation [30] of partial solutions for each group of 2^k elements with nonzero coefficients in the expansion of M. Possible scattering by the boundaries of the computation region was suppressed by utilising perfectly matched layer (PML) boundary conditions [33]. In our case, we used 11 absorbing PMLs with a total thickness of 0.5 μm.

Note that the analytical capabilities of the MoL ensure significant advantages over numerical methods of direct simulation as to computation efficiency. This enables exact results to be obtained in the case of multiple scattering even for weak tunnel coupling and extremely weak scattering (at a level of 10^{-10} and below relative to the incident power on each individual reflecting element).

Figure 1 illustrates the geometry of the tunnelling scattering of light by periodic polymer inserts. The arrows schematically represent the incident and reflected TE_0 fundamental

modes of the optical waveguide (shown at left) and scattered fields. The wavelength in our simulations was 1.55 μm, and we examined a standard silicon-on-insulator (SOI) structure in which a thin silicon optical waveguide was formed on a thick oxide layer 2 μm in thickness, with a refractive index of 1.447, situated on a silicon substrate (refractive index of 3.478). The period of the structure, 1.6 μm, corresponds to resonance tunnel coupling in the first order of diffraction ($p = 1$) for the incident wave of the silicon waveguide and the leaky wave of the segmented waveguide, propagating in the forward direction. The refractive index and thickness of the silicon wire (in the 2D approximation) are 3.0 and 0.22 μm. The refractive index and thickness of the polymer inserts are 1.521 and 1.1 μm, and those of the oxide buffer layer between them are 1.4 and 0.3 μm, respectively.

Figure 2 shows the spectral dependences of transmittance (T) and reflectance (R) calculated in a wide spectral range for the TE_0 fundamental mode by the method of lines. The calculation results indicate that the TE_0 mode coupled into the silicon waveguide can propagate with insignificant losses through a waveguide structure containing a large number of periodically arranged polymer tunnelling inserts. The only exception is a finite set of fixed wavelengths for which there is resonance Bragg scattering in different orders of diffraction into the guided TE_0 mode of the silicon waveguide ($\lambda_B = 1.5319$ and 1.8236 μm) and to the virtual leaky mode of the segmented waveguide ($\lambda_L = 1.52545$, 1.54983 and 1.94125 μm).

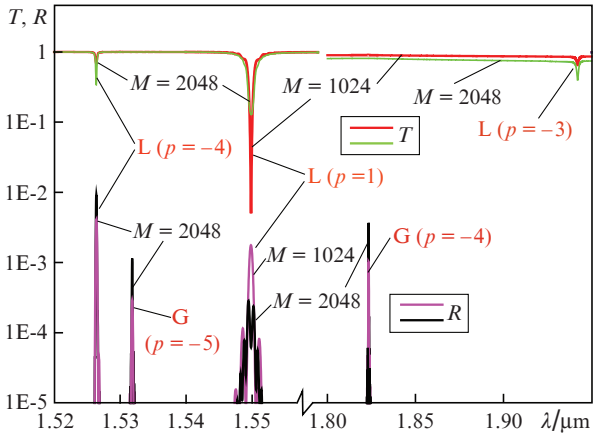

Figure 2. (Colour online) Spectral dependences of optical transmittance (T) and reflectance (R) for the TE_0 fundamental mode of an optical waveguide in the presence of different numbers ($M = 1024$ and 2048) of periodically arranged scattering dielectric polymer strips. We identified peaks corresponding to incident wave energy conversion to both the guided mode (G) and leaky wave (L) for various orders of the diffraction grating (p) (two-dimensional calculation by the method of lines).

Note that the periodically segmented polymer structure has a large period (1.6 μm), and the condition for strong scattering to radiation modes is fulfilled for it. Numerical simulation results for optical wave propagation through a separately located segmented waveguide demonstrate (Fig. 3) that, in contrast to subwavelength structures, it has a very high propagation loss (at least 70 dB cm^{-1} even beyond the Bragg blocking band; see the plateau in the central part of Fig. 3). Thus, it is not an optical waveguide in the ordinary sense of the word, but, as shown below, this segmented structure tunnel-coupled to a thin silicon wire acquires properties of a leaky waveguide capable of supporting the propagation of a localised optical mode whose energy is emitted as it propagates. Figures 4–9 illustrate this effect in greater detail.

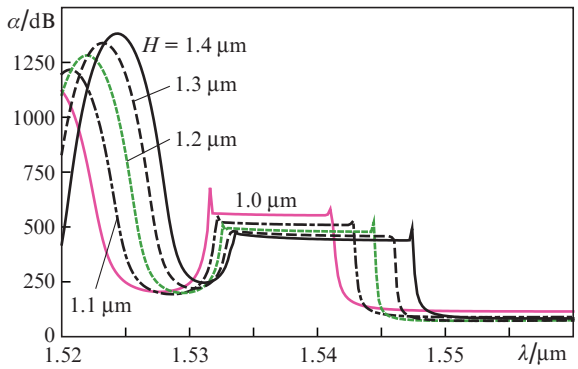

Figure 3. Spectral dependences of the loss α in a separately located segmented waveguide at various polymer core thicknesses H (two-dimensional calculation by the method of lines).

Figure 4 illustrates the spectral behaviour of the transmittance (T) and reflectance (R) for the TE_0 mode propagating in a silicon waveguide in the presence of a periodically segmented polymer structure of various thicknesses H. Note that the guided mode blocking level depends on the type of process (forward, i.e. $p = 1$, or backward, $p = -4$); the number of elements, M (the length of the segmented structure, L); and thickness H, which determines the wavelengths at which there is coherent conversion to leaky waves of different directions (Fig. 5). Using these data and the Bragg matching conditions for different orders of diffraction, p, we can determine the effective mode indices (N_L) of leaky waves in a segmented waveguide (Fig. 6).

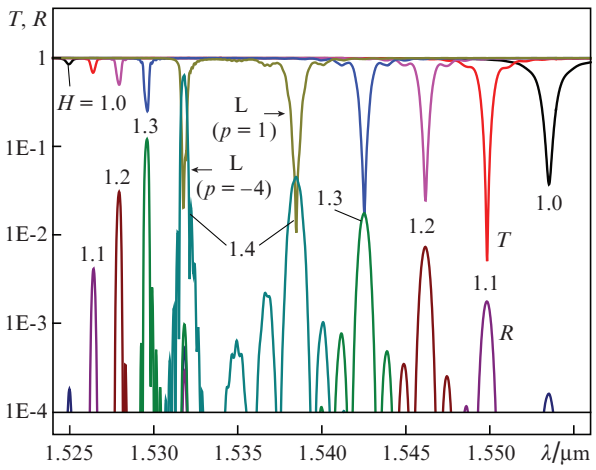

Figure 4. (Colour online) Spectral dependences of transmittance (T) and reflectance (R) for the TE_0 fundamental mode of an optical waveguide in the case of scattering to a leaky wave at various thicknesses H of a segmented waveguide with $M = 1024$ (two-dimensional calculation by the method of lines).

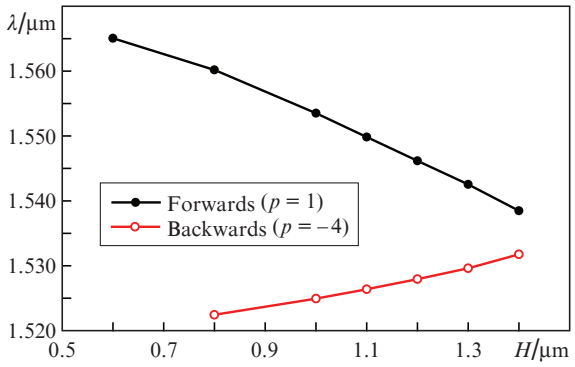

Figure 5. Blocking wavelength as a function of segmented waveguide thickness for the TE_0 fundamental mode under resonance conditions between the mode of the silicon wire and the segmented waveguide's virtual leaky mode propagating forwards ($p = 1$) and backwards ($p = -4$) at different orders of diffraction, p; $M = 1024$, buffer layer thickness $d = 0.3$ μm (two-dimensional calculation by the method of lines).

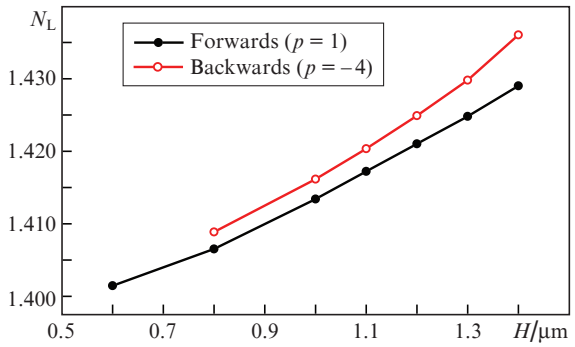

Figure 6. Effective mode index as a function of the thickness of periodic polymer strips for a virtual leaky mode of a segmented waveguide; $M = 1024$, buffer layer thickness $d = 0.3$ μm (two-dimensional calculation by the method of lines).

Under nearly optimal conditions for conversion to a forward leaky wave ($p = 1$, $H = 1.0$ and 1.1 μm), we observe an abnormally strong guided mode transmission signal suppression at an extremely low backreflection level (abnormal blocking effect). Conversion to a backward leaky wave occurs in a high order of diffraction ($p = -4$) and, at the structural parameters used by us, has lower efficiency and a high level of parasitic scattering to the backward guided mode. For this reason, we concentrate here on a more efficient conversion to a forward leaky wave, for which the period of the structure was chosen to be 1.6 μm, which ensures phase matching between interacting waves in the telecom range in the first order of diffraction ($p = 1$).

To gain greater insight into this unusual effect, we constructed images of total optical fields for two closely spaced optical wavelengths. For one wavelength (Fig. 7, $\lambda = 1.54983$ μm), there is a strong guided mode propagation blocking due to the efficient grating-induced coupling of the guided mode of the parent waveguide with the leaky wave of the segmented waveguide. At a number of periodic segments $M = 1024$, near the optimal value $M_{opt} = 950$ (for $H = 1.1$ μm and $d = 0.3$ μm), most of the energy of the guided wave converts to the leaky wave and then converts to radiation modes or is emitted through the end face of the segmented structure (Figs 7a, 7b). At the larger number of segments ($M = 2048$), the incident wave energy 'passes' twice upwards and downwards between the conventional and segmented waveguides (Fig. 7c), but, because of the loss due to the emission of the virtual leaky mode (above), the residual energy of the wave in the silicon wire (below) is considerably lower than the initial energy of the incident wave. As mentioned above, the phenomenon has a resonant character.

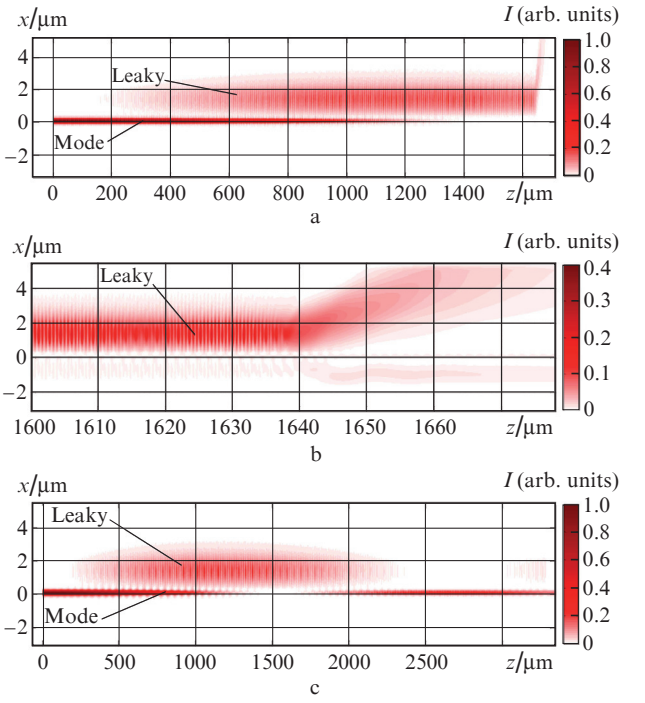

Figure 7. (Colour online) Spatial electromagnetic field density distributions for resonance conversion of the guided TE_0 mode (Mode) to a leaky wave (Leaky) of a segmented waveguide ($\lambda = 1.54983$ μm, $p = 1$): (a) total field at $M = 1024$, (b) detailed field distribution at the right-hand end of the structure for $M = 1024$, (c) total field at $M = 2048$. Two-dimensional calculation by the method of lines, $H = 1.1$ μm, $d = 0.3$ μm.

Next, we slightly shifted the operating wavelength (by 0.001 μm) (Fig. 8), which led to drastic changes in the field density distribution. The shift caused a deviation from the Bragg conditions of matching with a virtual leaky wave and, as a consequence, the conversion of the guided mode energy in the silicon wire to the virtual mode energy dropped sharply. As a result, we observed efficient TE_0 wave transmission under the segmented structure, accompanied by slight attenuation (caused by a weak coupling with radiation modes), whose magnitude was determined by the thick tunnel buffer layer ($d = 0.3$ μm) between the parent waveguide (below) and the segmented structure (above).

To independently verify the results obtained by the semi-analytical method of lines, we carried out a similar analysis using the finite-difference time-domain method [28], which can be considered to a certain extent as a numerical experiment. Figure 9 compares the results obtained for our 256-segment structures by the method of lines and the FDTD method. It is seen that the spectral dependences of the coefficients R and T are very similar in shape. In particular, they

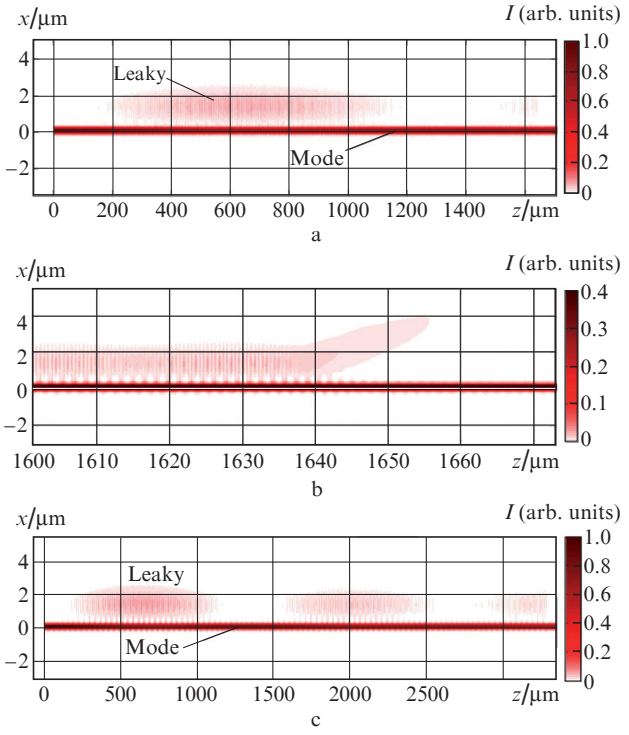

Figure 8. (Colour online) Spatial electromagnetic field density distributions for nonresonant conversion of the guided TE_0 mode (Mode) to a leaky wave (Leaky) of a segmented waveguide ($\lambda = 1.54883$ μm, $p = 1$): (a) total field at $M = 1024$, (b) detailed field distribution at the right-hand end of the structure for $M = 1024$, (c) total field at $M = 2048$. Two-dimensional calculation by the method of lines, $H = 1.1$ μm, $d = 0.3$ μm.

demonstrate an abnormal blocking effect (sharp dips in the transmitted wave) at a low level (under –25 dB) of the reflected reverse wave to the fundamental mode of the silicon wire. It is well seen that, in the case of Bragg diffraction ($\lambda \sim 1.53$ μm) into the backward guided mode, there is a simultaneous decrease in the power of the transmitted wave (T) and a comparable increase in the power of the reflected wave (R), just as in Fig. 4.

Note the slight difference in the position of the peak of the resonant blocking of the transmitted wave, which is attributable to the common shift of the curves because of the finite computation grid step (40 nm) in the FDTD method. In this sense, from the viewpoint of the application of numerical methods, the modelled structures are not absolutely identical. Because of the difference in computation grid step, the effective refractive indices of optical modes differ slightly (by 0.33%) and the spectral curves are displaced as a whole relative to each other, without changes in the mutual arrangement of the peaks. Because of this, as a result of the slight distinction between the effective refractive indices, phase matching conditions are observed at slightly different wavelengths, as illustrated by Fig. 9. This distinction is not critical and decreases with decreasing computation grid step, but this is accompanied by a considerable increase in computation time and required RAM, which is especially critical for the FDTD method at the large dimensions of the structure that were used in our numerical experiments.

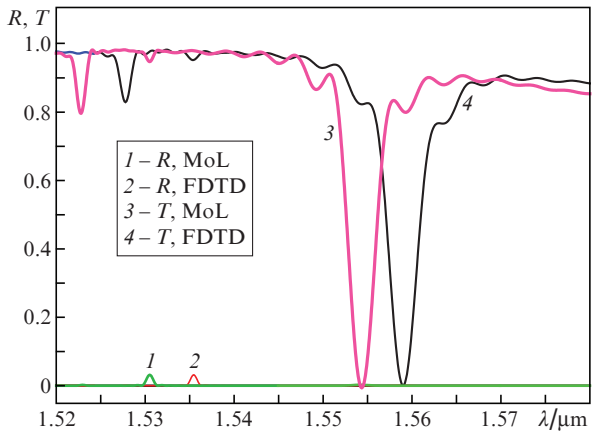

Figure 9. (Colour online) Spectral dependences of optical transmittance (T) and reflectance (R) for an optical waveguide with periodic tunnelling inserts; $M = 256$ (two-dimensional calculations by the method of lines and the FDTD method; $d = 0.1$ μm).

The minimum in transmittance is observed at the optimal number of segments $M_{opt} = 950$, which is smaller than that in the structure simulated by us. We carried out an additional analysis and optimisation of the parameters of the band rejection filter based on the proposed periodically segmented structure, optimised the number of segments for each group of parameters and determined the key parameters of the filter: rejection rate, rejection and parasitic backscatter levels for the fundamental mode, and blocking frequency band at various decibel levels ($\Delta\lambda_{3\,dB}$, $\Delta\lambda_{10\,dB}$ and $\Delta\lambda_{20\,dB}$) (Table 1). It is well seen that, varying parameters of the structure, one can change the rejection bandwidth by approximately a factor of 5, while maintaining the low level of parasitic signals (under –40 dB). Increasing the length of the structure reduces the filtering bandwidth, but only to a certain level, starting at which a limitation on the linewidth begins to show up due to the high attenuation level (above 70 dB) of the leaky wave of the segmented waveguide. Note

Table 1. Principal parameters of optical band rejection filters based on structures with various buffer layer thicknesses d.

d/μm	$\Delta\lambda_{3\,dB}$/nm	$\Delta\lambda_{10\,dB}$/nm	$\Delta\lambda_{20\,dB}$/nm	λ/μm	T/μm	R/μm	M_{opt}	L/mm	$\Delta\lambda_{3\,дБ}L$/mm^2	N_L
0.1	4.32	1.52	0.5	1.55946	47.6	41.1	317	0.51	2.19	1.40726
0.2	2.62	0.87	0.28	1.55600	58.4	41.9	611	0.98	2.56	1.410849
0.3	1.57	0.49	0.15	1.55345	43.1	44.7	1280	2.05	3.22	1.413491
0.4	0.85	0.26	0.09	1.55133	45.5	47.3	2767	4.43	3.76	1.415688
0.5	0.6	0.22	0.08	1.54960	79.6	62.4	9020	14.43	8.66	1.417482
0.4*	0.82	0.25	0.075	1.55069	45.1	46.1	2767	4.43	3.63	1.416088

* The refractive index of the medium around the polymer inserts was changed by 0.001 (from 1.4 to 1.401) in order to demonstrate the use of the filter as an optical sensor.

that the proposed type of optical band rejection filter has a very broad free spectral range (above 290 nm), which is limited from below by parasitic scattering to a leaky wave (λ = 1.526 μm) and the backward guided mode (λ = 1.532 μm) and from above by possible processes in high orders of diffraction (at wavelengths above 1.823 μm), as illustrated in Fig. 3.

Also presented in Table 1 are illustrative data on the use of the proposed filter as an optical sensor at H = 1 μm. To assess its sensitivity, we calculated the properties of the sensor at different refractive indices of the medium around the segmented structure (n = 1.4 and 1.401, Δn = 0.001) and determined the filtering frequencies and effective refractive index N_L of the segmented waveguide. Next, using these data we found that the relative sensitivity to changes in refractive index was $\Delta N_L/\Delta n$ = 0.4 and that to changes in wavelength was $\Delta\lambda/\Delta n$ = 0.63 μm. Note that these values are approximately twice those of the sensitive part of silicon wire-based sensors and approach those of slot waveguides with a slot width under 100 nm [34]. Since sensors based on segmented waveguides are substantially easier to fabricate than slot waveguides, the structures under investigation are potentially attractive as well for use as optical sensors.

One point that we believe to be of critical importance is worthy of special attention. The observed phenomenon, which we refer to as abnormal blocking, has many features in common with the conversion of a guided mode to a leaky wave in a fibre configuration as a result of the diffraction from long-period gratings in optical fibres [35, 36] or diffraction from an acoustic wave into a leaky wave [37, 38] of an anisotropic waveguide in lithium niobate [39–41]. The described phenomenon is abnormal in that, in an ordinary situation, the presence of a diffraction grating in the form of tunnel-coupled periodic dielectric inserts near the optical waveguide leads to diffraction into waves that already exist in the structure without a given perturbation (in the form of a diffraction grating). In particular, in the case of an optical waveguide this may be resonant conversion to a backward guided mode (as in a band rejection filter) or broadband diffraction into radiation modes (as in grating coupling elements). In our case, the presence of a segmented diffraction grating over a silicon wire produces a new tunnel-coupled structure, namely, a virtual leaky waveguide, which has its own propagation characteristics, field distribution and attenuation, differing from the attenuation in an analogous segmented structure with no silicon wire. It is with this leaky mode, which does not exist without tunnel coupling between the segmented and waveguide structures, that we consider the interaction of the guided mode of the silicon wire.

In this sense, this phenomenon can be referred to as 'abnormal', because it has not been observed previously in a standard optical waveguide configuration with a diffraction grating and exhibits properties atypical of diffraction into radiation modes. It is characteristic of a different type of structure, containing an additional waveguide, which is initially missing in our interaction configuration.

3. Conclusions

Results of numerical simulation by the high-accuracy method of lines (MoL) indicate that collective scattering of a guided mode by a large number of periodic segmental inserts tunnel-coupled to the parent optical waveguide may lead to an abnormal blocking of the guided mode. In contrast to broadband diffraction into radiation modes by a grating coupling element, the interaction has a resonant character. Moreover, in contrast to the known narrow-band Bragg reflection effect, there is no backward reflected guided mode, and all energy is emitted to space through resonant tunnel coupling with a virtual leaky wave belonging to the entire structure of periodic segments with the silicon wire. In our case, the segmental part of the structure has the form of a thick (H = 1.0–1.1 μm) SU-8 polymer layer, in which deep, 0.8-μm-long grooves spaced 1.6 μm apart are produced by etching. The segmental part is located over a 0.22-μm-thick silicon wire in an SOI structure with a 2-μm-thick buried oxide layer and is separated from the waveguide by a 0.1- to 0.4-μm-thick buffer layer.

The abnormal blocking of the guided mode on account of the weak tunnel coupling with a large number of periodically arranged strips operating as a virtual segmented leaky waveguide should be taken into account in designing and investigating photonic structures with a large number of tunnelling scattering elements. In particular, it can be successfully used in designing band rejection filters [24] with a low backscatter level and sensing elements, as well as in analysing multiple crossings of low-dimensional waveguides in high refractive index contrast structures [7–9].

Acknowledgements. This work was supported by the Russian Foundation for Basic Research (Grant No. 15-07-03617-a). We are grateful to Synopsys, Inc. for providing RSoft programmes for our optical computations [32].

References

1. Tamir T., in *Topics in Applied Physics* (Berlin: Springer, 1975; Moscow: Mir, 1978).
2. Hunsperger R.G. *Integrated Optics: Theory and Technology* (Berlin: Springer, 1984; Moscow: Mir, 1985).
3. Soref R. *IEEE J. Sel. Top. Quantum Electron*., **12**, 1678 (2006).
4. Jalali B., Fathpour S. *J. Lightwave Technol.*, **24**, 4600 (2006).
5. Reed G.T. *Silicon Photonics. The State of the Art* (Chichester: John Wiley & Sons, 2008).
6. Roelkens G., Dumon P., Bogaerts W., van Thourhout D., Baets R. *IEEE Photonics Technol. Lett*., **17**, 2613 (2005).
7. Tsarev A.V. *Opt. Express*, **19**, 13732 (2011).
8. Tsarev A.V., Kolosovskii E.A., *Kvantovaya Elektron*., **43**, 744 (2013) [*Quantum Electron*., **43**, 744 (2013)].
9. Tsarev A. *IEEE J. Sel. Top. Quantum Electron*., **20**, 77 (2014).
10. O'Faolain L., Tsarev A. *Opt. Lett*., **39**, 3627 (2014).
11. Marcuse D. *J. Lightwave Technol*., **LT-5**, 268 (1987).
12. Zhang Sh., Tamir Th. *Opt. Lett*., **22**, 1159 (1997).
13. Kolosovsky E., Tsarev A. *Abs. 22th Intern. Workshop Opt. Wave & Waveguide Theory and Numerical Modelling (OWTNM 2014)* (Nice, France, 2014, P-09) p. 52.
14. Halir R. et al. *Laser Photonics Rev*., **9**, 25 (2014).
15. Tong X. C. *Advanced Materials for Integrated Optical Waveguides* (London: Springer Intern. Publ., 2014) Vol. 46, pp 509–543.
16. Liu J. et al. *RSC Adv.*, **5**, 15784 (2015).
17. Denisyuk I.Yu., Burunkova Yu.E., Pozdnyakova S.A., et al. *Opt. Spektrosk*., **119**, 691 (2015).
18. Passaro V.M.N. *J. Lightwave Technol.*, **18**, 973 (2000).
19. Taillaert D., Bienstman P., Baets R. *Opt. Lett*., **29**, 2749 (2004).
20. Doylend J.K., Knights A.P. *IEEE J. Sel. Top. Quantum Electron*., **12**, 1363 (2006).
21. Tsarev A.V. *Opt. Express*, **17**, 13095 (2009).
22. Jewell J.L., Harbison J.P., Scherer A., Lee Y.H., Florez L.T. *IEEE J. Quantum Electron*., **27**, 1332 (1991).
23. Coldren L.A. *IEEE J. Sel. Top. Quantum Electron*., **6**, 988 (2000).

24. Weber J.-P., Stoltz B., Dasler M., Koek B. *IEEE Photonics Technol. Lett*., **6**, 77 (1994).
25. Ahn S.-W., Shin S.-Y. *IEEE J. Sel. Top. Quantum Electron*., **75**, 819 (2001).
26. Kwon M.-S., Shin S.-Y. *J. Lightwave Technol*., **22**, 1968 (2004).
27. Chiang K.S. *Appl. Opt.*, **25**, 2169 (1986).
28. Rogge U., Pregla R. *Opt. Soc. Am. B*, **8**, 459 (1991).
29. Scarmozzino R., Gopinath A., Pregla R., Helfert S. *IEEE J. Sel. Top. Quantum Electron*., **6**, 150 (2000).
30. Jamid H.A., Akram M.N. *J. Lightwave Technol.*, **20**, 1204 (2002).
31. Yee K.S. *IEEE Trans. Antennas Propag*., **AP-14**, 302 (1966).
32. https://optics.synopsys.com/rsoft/.
33. Huang W.P., Xu C.L., Lui W., Yokoyama K. *IEEE Photonics Technol. Lett*., **8**, 649 (1996).
34. La Notte M., Passaro V.M. *Sens. Actuators, B*, **176**, 994 (2013).
35. Erdogan T. *J. Opt. Soc. Am. A*, **14**, 1760 (1997).
36. Ivanov O.V., Nikitov S.A., Gulyaev Yu.V. *Usp. Fiz. Nauk*, **176**, 175 (2006).
37. Petrov D.V., Chtyroki I. *Kvantovaya Elektron*., **12**, 987 (1985) [*Sov. J. Quantum Electron*., **15**, 650 (1985)].
38. Petrov D.V., Tsarev A.V., Yakovkin I.B. *Kvantovaya Elektron*., **15**, 173 (1988) [*Sov. J. Quantum Electron*., **18**, 110 (1988)].
39. Yamanouchi K., Kamiya T., Shibayama K. *IEEE Trans. Microwave Theory Tech*., **26**, 298 (1978).
40. Čtyroký J., Čada M. *Opt. Commun*., **27**, 353 (1978).
41. Kolosovsky E.A., Petrov D.V., Tsarev A.V., Yakovkin I.B. *Opt. Commun*., **43**, 21 (1982).